J Biomol NMR (2010) 47:283–288
DOI 10.1007/s10858-010-9426-8

NMR STRUCTURE NOTE

NMR structure note: solution structure of the core domain of MESD that is essential for proper folding of LRP5/6

Jianglei Chen · Qianqian Li · Chia-Chen Liu · Bei Zhou · Guojun Bu · Jianjun Wang

Received: 26 April 2010 / Accepted: 11 May 2010 / Published online: 27 May 2010

Biological context

Low-density lipoprotein receptor (LDLR) family controls diverse developmental and physiological pathways, including an endocytic cargo function and signaling capacities (Herz and Bock 2002). LDLR family members belong to type I transmembrane proteins that contain repeating modules, including the cysteine-rich repeats (LDL-A), making up the ligand-binding domains, a BP domain formed by six YWTD repeats (β-propeller) and an epidermal growth factor (EGF) repeat. The number and arrangement of these modules vary among family members. LRP5/6, a co-receptor for binding to Wnts in the Wnt signaling pathway, start with a BP domain, which repeats four times, followed by three LDL-A repeats. The extracellular side is anchored on the plasma membrane by a single transmembrane segment, followed by a cytoplasmic tail containing NPXY signals for endocytosis and interaction motifs for a variety of cytoplasmic adaptor and scaffolding proteins (Strickland et al. 2002).

An ER-resident specialized chaperone, termed *mesoderm development* (MESD) in mouse (Hsieh et al. 2003) and *boca* in *Drosophila* (Culi and Mann 2003), is essential for the folding and intracellular trafficking of LRP5/6. Boca is specifically required for maturation of the BP domains of LpR2, which is the *Drosophila* homologue of LDLR (Culi et al. 2004). A lethal W32R mutation of *boca* ($boca^1$ allele) can be rescued by the expression of a wild-type *boca* cDNA, suggesting that this mutation is a loss-of-function mutation (Culi and Mann 2003). It is suggested Boca directly binds to the newly synthesized, nascent β-propeller domain, maintaining it in an interaction competent state for binding of the newly synthesized, adjacent EGF-repeat. Upon EGF-binding, the BP domain achieves a proper fold, subsequently eliminating Boca-binding (Culi et al. 2004). We showed that a vertebrates homologue of Boca, MESD(12–155), fails to bind to mature, membrane-associated LRP6, whereas the C-terminal region, MESD(150–195), which is absent in Boca, is sufficient for binding to the properly folded, mature LRP6 (Li et al. 2005). These results suggest that MESD(12–155) only binds to unfolded BP-domains of LRP5/6 to promote their folding. Once the BP domains fold properly, MESD(12–155) dissociates from the mature BP domain (Culi et al. 2004). Thus, MESD(12–155) may serve as a chaperone domain of MESD for proper folding of the BP domains of LRP5/6. The NMR structure of a MESD truncation mutant, MESD(60–155) showed a structured core region of a four-stranded anti-parallel β-sheet and three α-helices positioned in one side of the sheet (Kohler et al. 2006). This structure lacks the first 59-residues, thus can't be used to provide structural basis of the lethal $boca^1$ allele which

The PDB accession code of the NMR structure of MESD(12–155): 2KMI.

Electronic supplementary material The online version of this article (doi:10.1007/s10858-010-9426-8) contains supplementary material, which is available to authorized users.

J. Chen · Q. Li · J. Wang (✉)
Department of Biochemistry and Molecular Biology, School of Medicine, Wayne State University, Detroit, MI 48201, USA
e-mail: jjwang@med.wayne.edu

C.-C. Liu · G. Bu
Departments of Pediatrics, and Cell Biology and Physiology, School of Medicine, Washington University, St. Louis, MO 63110, USA

B. Zhou
Department of Biochemistry, Duke University Medical Center, Durham, NC 27710, USA

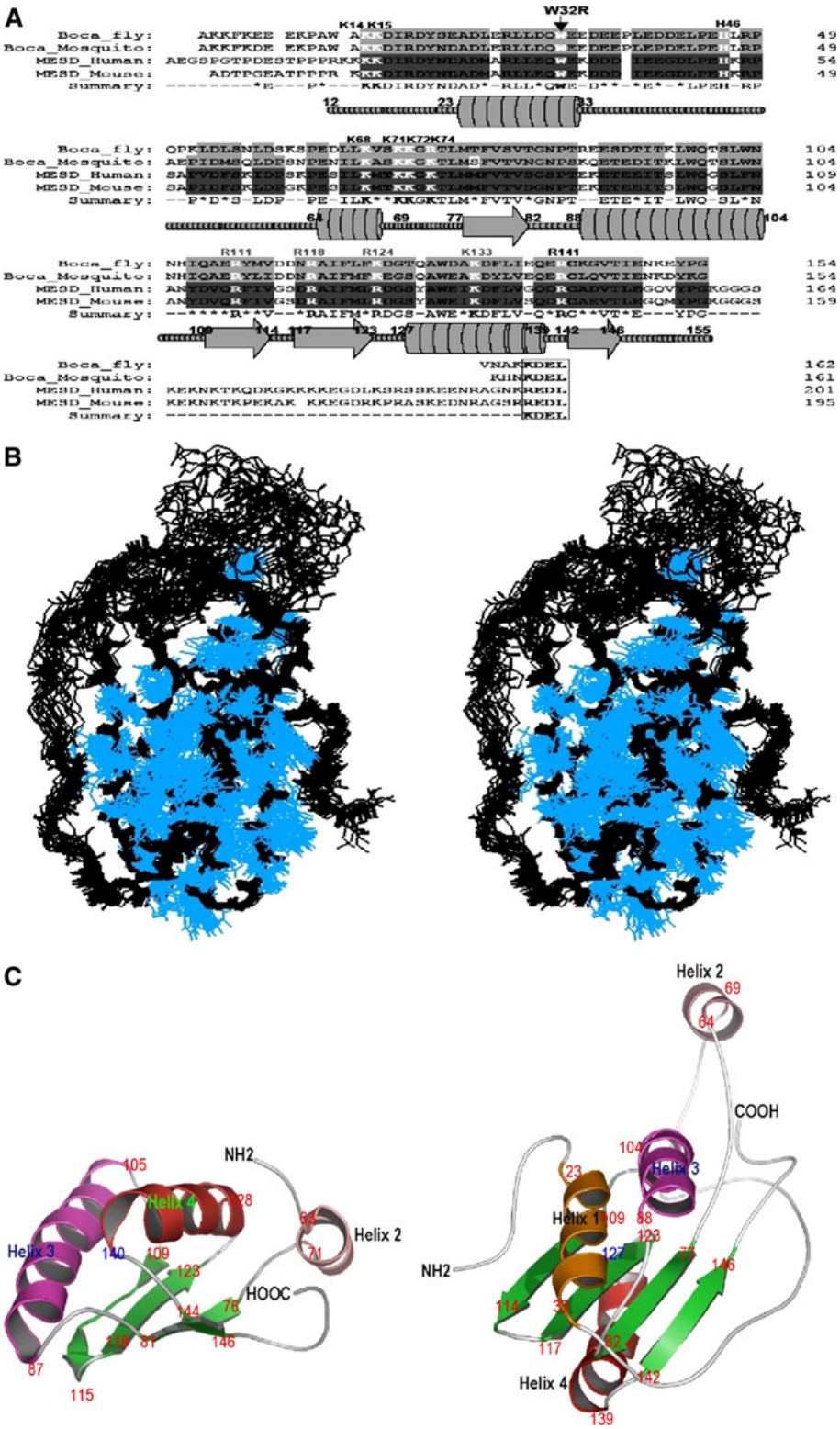

Fig. 1 **a** Sequence alignment of MESD and Boca from four species. The conserved residues are highlighted in *gray*. The conserved lysine, histidine and arginine residues are colored in *white* letter and labeled on top of the sequence. *Black*-labeled residues are solvent exposed whereas *grey*-labeled residues are buried. The secondary structures based on NMR structure of MESD(12–155) are displayed under the sequence. **b** 20 best-fit NMR structures of MESD(12–155). The backbone atoms are in *black* and the heavy atoms of the sidechain are in *blue*. **c** A structural comparison of the published NMR structure of MESD(60–155) and the NMR structure of MESD(12–155). The secondary locations are labeled by *red* numbers as the residue numbers

contains the loss-of-function W32R mutation. Functional data confirmed a structural core domain, suggesting that both the N- and C-termini unstructured regions of MESD were required to facilitate maturation of LRP6 on the cell surface (Koduri and Blacklow 2007).

The structure of MESD(12–155) is critical for us to understand the chaperone function of MESD. We solved the NMR structure of MESD(12–155), showing a tightly packed core structure that is centered at a four stranded, anti-parallel β-sheet, surrounded by two helices on the top and one helix in

the bottom. An additional flexible helix (residue 64–69) is located in a long loop (residues 33–77) containing several conserved lysine residues, K68/K71/K72/K74 and the conserved H46, the only histidine in MESD. Chemical shift mapping indicates the W32R mutation causes major chemical shift changes of residues 43–48 and 68–76, suggesting that these two regions are likely critical to MESD's chaperone function. Chemical shift mapping between MESD and MESD(12–155) further indicates major chemical shift changes in residues 68–76, suggesting its potential interactions with the C-terminal domain of MESD.

Materials and methods

Site-directed mutagenesis

Site-directed mutagenesis was carried out using the QuickChange™ mutagenesis kit (Stratagene, CA). The mutations were confirmed by DNA sequencing.

NMR spectroscopy and structure determination

The NMR sample contained 1 mM isotope-labeled MESD protein, 25 mM sodium phosphate at pH 6.8, 0.01 mM NaN_3, 10 mM EDTA, 20 mM d_{10}-DTT, 0.03 mM DSS and 10% D_2O. All spectra were acquired at 30°C on a 600 MHz Varian INOVA spectrometer equipped with a cryogenic probe. 3D-HNCACB, CBCA(CO)NNH and HNCO spectra were used for backbone atom assignment while HCC-TOCSY-NNH, CCC-TOCSY-NNH and ^{15}N-edited NOESY were collected for the sidechain atom assignment (Clore and Gronenborn 1991). The NMR data was processed using nmrPipe (Delaglio et al. 1995) and analyzed on a SGI workstation using PIPP (Garrett et al. 1991) and NMR view (Johnson 2004). TALOS program was used to obtain the backbone dihedral angles (ϕ and ψ based on chemical shift information (Cornilescu et al. 1999). NOE distance restraints were generated using 3D ^{15}N-edited NOESY and 4D ^{15}N/^{13}C-edited NOESY experiments. NMR restraints included: 216 dihedral angle constraints, 1,156 distance constraints and 34 constraints for hydrogen bonds, and were used as input for CYANA calculations (Guntert 2004). Two hundred structures were generated and energy minimized in CYANA, including 10,000 steps of simulated annealing. Final NMR structures were analyzed using InsightII (MSI, San Diego) and PROCHECK (Laskowski et al. 1993).

Results and discussion

Sequence alignment between vertebrate MESD and invertebrate Boca indicates a high sequence homology for residues 12–155 (Fig. 1a). However, Boca lacks the C-terminal fragment (residues 155–191) of MESD. MESD (12–155) represents the Boca sequence in vertebrate species, suggesting MESD(12–155) may serve as an independent structural domain that performs the same chaperone function as Boca for the proper folding of LRP5/6. We determined NMR structure of MESD(12–155). An overlay of the 20 best-fit NMR structures of MESD(12–155) are shown in Fig. 1b. Table 1 lists structural statistics for the ensemble of 20 structures. The RMSD of the backbone heavy atoms of the rigid secondary structure region is 0.42 ± 0.04 Å, whereas the RMSD of all heavy atoms for the same region is 1.10 ± 0.09 Å. The precision of this NMR structure allows us to accurately analyze the side chain conformations of the key residues. PROCHECK analysis indicates that in addition to 14 Gly and 11 Pro residues, 90 residues (75.6%) are located in the most favored regions, 25 residues (21.0%) are in the additional allowed regions, 4 residues (3.4%) are in the generously allowed region of the Ramachandran plot.

The average NMR structure of MESD(12–155) is displayed in ribbon diagram (Right, Fig. 1c). It centers at a

Table 1 Structural statistics of the 20 best-fit NMR structures of MESD(12–155)

Number of NMR restraints	
Total NOE restraints	1,156
Intra-residue	110
Sequential ($\|i-j\| = 1$)	320
Medium range ($1 < \|i-j\| < 5$)	378
Long range ($\|i-j\| > 5$)	348
Number of Dihedral angle restraints	
ϕ	109
ψ	107
Number of hydrogen bond restraints	34
Structural Statistics	
Distance violations (>0.1Å, %)	0.25
Distance violations (>0.2 Å)	1
Average Distance violations ± rmsd	0.0075 ± 0.0017
Dihedral angle violations (>2.5°,%)	0.0046
Dihedral angle violations (>5°)	0
Average Dihedral angle violations ± rmsd	0.2083 ± 0.0702
Ramachandran plot (%)	
Residues in most favored regions	75.1
Residues in additional allowed regions	21.3
Residues in generally allowed regions	3.6
Residues in disallowed regions	0.0
Average pairwise r.m.s.d (Å) (20 structures, residues 23–33, 77–82, 88–104, 109–114, 118–122, 128–139, 142–146)	
Backbone heavy atoms	0.42 ± 0.04
All heavy atoms	1.10 ± 0.09

four anti-parallel β-sheet, which is surrounded by three helices on the top (Helices 1–3) and one helix under the sheet (Helix 4). We carefully compared our NMR structure with the published NMR structure of MESD(60–155) (Kohler et al. 2006) (Left, Fig. 1c). A major tertiary structural difference is observed. In MESD(60–155), all three helices are located on the top of β-sheet. In contrast, only helices 1 and 3 are on the top and helix 4 is under the sheet in MESD(121–55). Surprisingly, the flexible short helix 2 is presented at a more distant position from the rest of the molecule, which is also distinctly different from helix 2 in MESD(60–155). In addition, the critical residue, W32, is located in helix 1 in MESD(12–155), whereas MESD(60–155) does not contain this residue (Fig. 2).

The electrostatic potential was calculated using the APBS program (Baker et al. 2001) and displayed using the Pymol program (DeLano Scientific, San Carlos) with the positive charged surface in blue and negatively charged surface in red (Fig. 2a). It can be clearly visualized that the MESD(12–155) structure contains two major positively charged surface areas. One area contains residues K14 and K15 on the N-terminal unstructured region and the other contains residues K68, K71, K72 and K74 which are located on helix 2 (K68) and in the loop region right after helix2. These lysine residues are conserved across Boca and MESD sequences (Fig. 1a). The only histidine of MESD/Boca, H46, is also surface located in a flexible loop connecting helices 1 and 2. W32, the functionally critical residue, is located in the C-terminus of helix 1 followed by a cluster of conserved negatively charged residues. Figure 2b summarizes these results by highlighting the most conserved lysine residues, H46 and W32. These conserved lysine residues, along with H46 and W32, are located on the outside edges of the same face of MESD(12–155), which may serve as the folding template for proper folding of the BP domain of LRP5/6. We suggest they are potential critical residues for the chaperone function of MESD(12–155).

To explore the structural basis of loss-of-function of the W32R mutant, we performed biophysical and NMR studies. Circular dichroism results indicate the W32R have nearly identical secondary structure and stability as those of wild-type MESD(12–155) (data not shown), suggesting loss-of-function of the W32R mutant may be due to tertiary structural changes of the mutant. NMR chemical shift mapping reveals significant spectral differences in the center of the spectra, even though a similar overall spectral pattern is observed between MESD(12–155) and

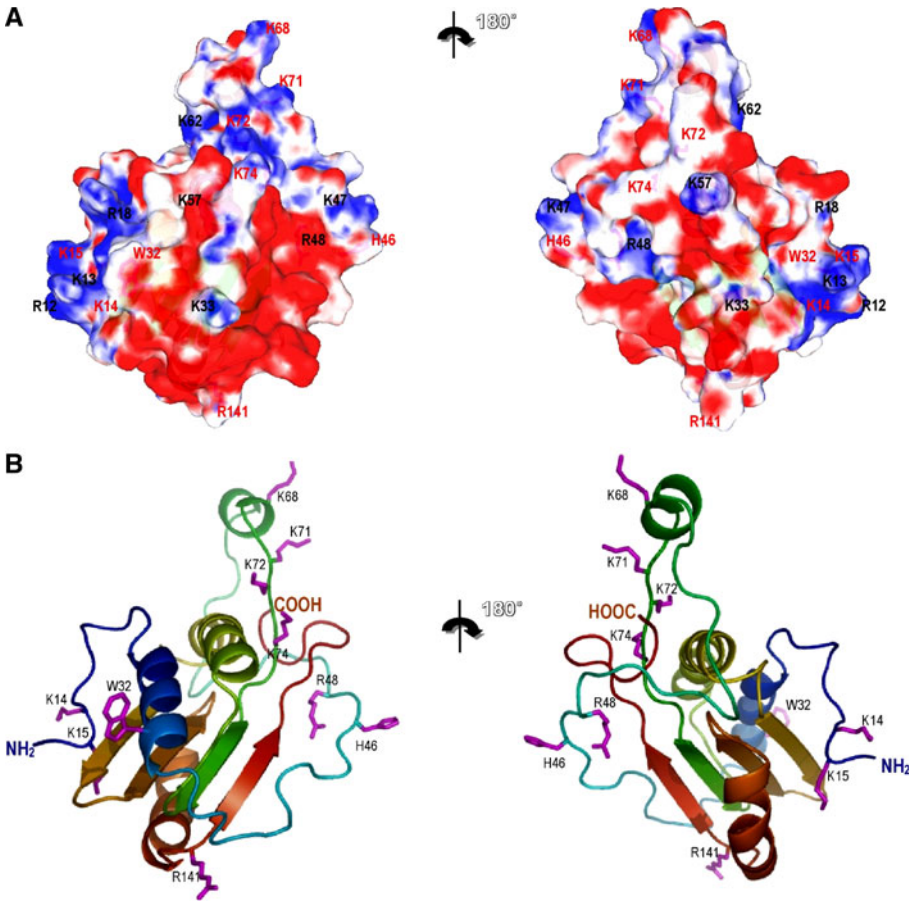

Fig. 2 **a** Electrostatic surface representation of MESD(12–155). Positively charged surface is in *blue* and negatively charged surface is in *red*. The conserved, surface located lysines, H46 and W32 are labeled in *red*, whereas the non-conserved lysines and arginines are labeled in *black*. **b** Ribbon diagram of MESD(12–155) at the same orientation as (**a**). Only conserved, surface located lysines, H46 and W32 are labeled

MESD(12–155)_W32R (Fig. 3a, b). We illustrated these results using MESD(12–155) structure (Fig. 3c). Clearly, the W32R mutation (labeled in red) causes unexpected but specific large chemical shift changes in two regions, residues 43–48 (labeled in pink) and residues 64–79 (labeled in green). Both regions are in the opposite end and far away from the W32R mutation. They are also located in the flexible loops and short helix 2 that contain conserved H46, K68, K71, K72 and K74. The third region with noticeable chemical shift changes is in residues 120–132 on strand 3 and helix 4 (labeled in brown). Strand 3 is positioned in a close distance with helix 1, where the W32R mutation is

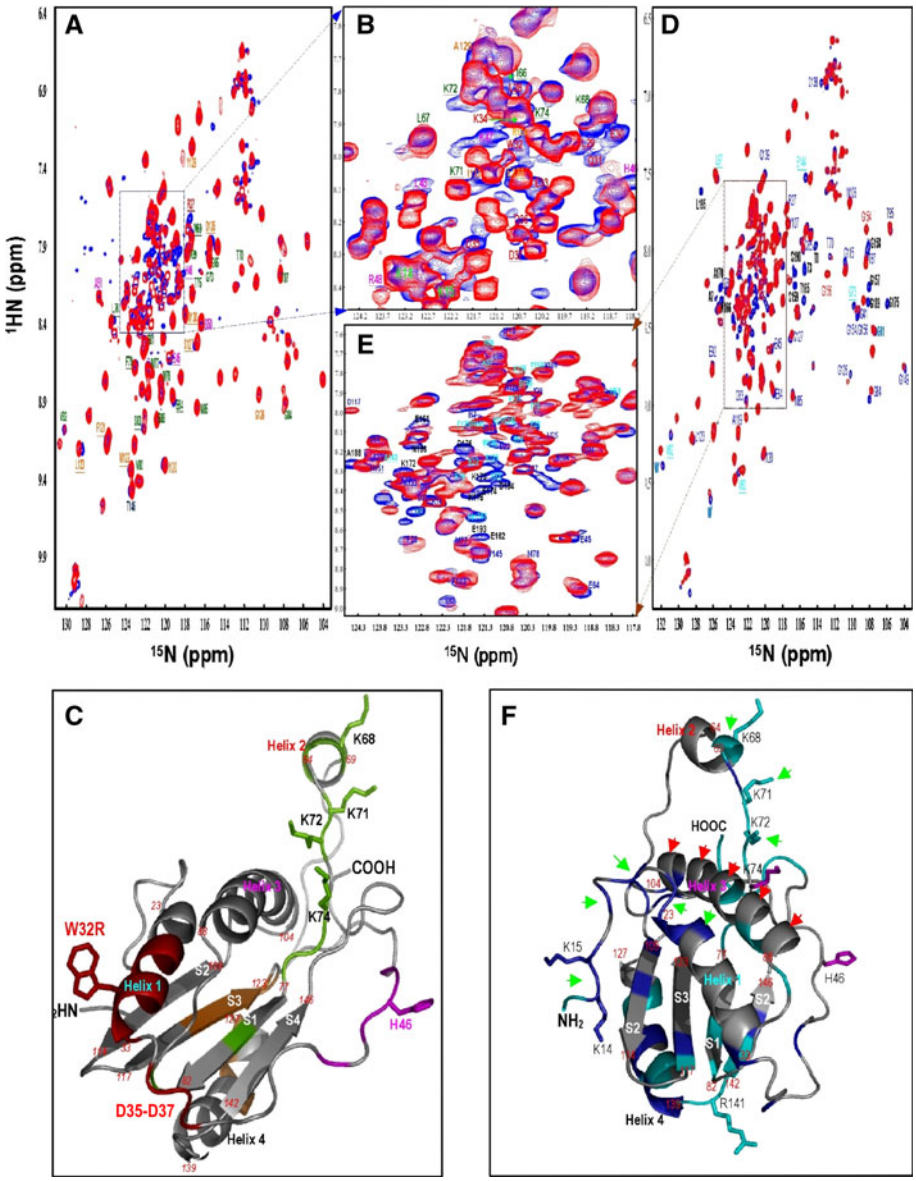

Fig. 3 **a–c** Chemical shift mapping between MESD(12–155) and MESD(12–155)_W32R. **a** ^{15}N–^{1}H HSQC spectral superposition of MESD(12–155) (*blue*) and MESD(12–155)_W32R (*red*). **b** The zoom-in view of the boxed region in A. The assignment is labeled next to the crosspeak and colored in different colors for different regions that display chemical shift changes. *Pink*: residues 43–48; *Green*: residues 64–79; *Brown*: residues 120–132. **c** NMR structure of MESD(12–155), summarizing the chemical shift mapping result with the same color codes. **d–f** Chemical shift mapping between MESD(12–155) and MESD. **d** ^{15}N–^{1}H HSQC spectral superposition of MESD(12–155) and MESD. **e** The zoom-in region of the same HSQC spectrum. The assignment is labeled next to the crosspeak and colored in different colors for different regions. *Black*: separated crosspeaks of residues 1–11 and 156–195; *Blue*: residues that display chemical shift changes in the range of ^{15}N: 0.2 ppm < change < 0.5 ppm and/or ^{1}H: 0.05 ppm < change < 0.1 ppm; *Cyan*: residues that display chemical shift changes in the range of ^{15}N: change > 0.5 ppm and/or ^{1}H: change > 0.1 ppm. **f** NMR structure of MESD(12–155), summarizing the chemical shift mapping result with the same color codes. *Red arrows* point at outer surface of helix 3 with no chemical shift change observed, green arrows point out potential domain-domain interaction interface

located. Strand 3 is also adjacent to strand 1, which shows large chemical shift perturbation (labeled in green) and connects with the flexible loop that contains conserved K68, K71, K72 and K74. Thus, our chemical shift mapping indicates the W32R mutation causes local chemical environmental perturbation of strand 3 and helix 4, which transduce information of the W32R mutation to the remote regions of residues 64–76 via strand 1. Furthermore, three aspartic acids, D35, D36 and D37, also showed large chemical shift changes (labeled in red) and they are located on the long flexible loop where H46 is also located. The W32R mutation causes perturbation of D35, D36 and D37, which transduce this mutation information to the remote region of residues 43–48 (labeled in pink). Since the W32R is a loss-of-function mutant, the specific large chemical shift changes of the conserved residues 43–48 and 64–79 caused by the W32R mutation provide direct experimental evidence that these residues are critical for MESD's chaperone function. In MESD(60–155), helix 2 is located in a complete different location from that of MESD(12–155) and could not present these positive lysine residues, such as K68, K71, K72 and K74, at the specific tertiary positions, serving as a template to promote proper folding the BP domains of LRP5/6.

We performed a complete assignment of the NMR spectra of MESD, which is deposited in BMRB databank with an access code: BMRB 16213. Chemical shift mapping indicates observable chemical shift differences between MESD and MESD(12–155) (Fig. 3d, e). We labeled the MESD(12–155) structure with the crosspeaks that display smaller chemical shift changes in blue (^{15}N dimension: 0.2 ppm $<$ change $<$ 0.5 ppm; ^{1}H dimension: 0.05 ppm $<$ change $<$ 0.1 ppm) and label the crosspeaks that show larger chemical shift changes in cyan (^{15}N dimension: change $>$ 0.5 ppm; ^{1}H dimension: change $>$ 0.1 ppm) (Fig. 3f). Several regions display significant chemical shift changes, including N- and C- terminal R12-M25 and M151-K155; structural core region, V80-L97, N104-R111, D117-A119 and A129-E144; and flexible region, K68-L76. Among these regions, residues V80-L97, N104-R111, D117-A119, A129-E144 are in the β-sheet and helices 3 and 4. These regions are involved in the assembling of the structural core, which are buried and unlikely available for inter-domain interactions. Indeed, the residues with noticeable chemical shift changes in helices 3 and 4 are facing inwards, whereas the residues on the outer surface have no chemical shift changes (red arrows). In contrast, two major regions, R12-M25 and K68-L76, display major chemical shift changes and both regions are fully solvent exposed and available for interaction (green arrows) with the C-terminal fragment, residues 156–195, of MESD. They are also the regions containing those conserved lysine residues, including K14, K15, K68, K71, K72 and K74, that potentially critical to MESD's chaperone function.

In conclusion, NMR structure of MESD(12–155) indicates that conserved lysine residues, K14, K15, K68, K71, K72 and K74, along with W32 and H46 are potential critical residues for MESD's chaperone function. In addition, these conserved lysine residues are also potentially involved into MESD's domain-domain interactions.

Acknowledgments This work is supported by NIH RO1 grants (HL074365 and HL076620 to JW). The authors also thank Ms Victoria Murray for critical reading of the manuscript.

References

Baker NA, Sept D, Joseph S, Holst MJ, McCammon JA (2001) Electrostatics of nanosystems: application to microtubules and the ribosome. Proc Natl Acad Sci U S A 98:10037–10041

Clore GM, Gronenborn AM (1991) Structures of larger proteins in solution: three- and four-dimensional heteronuclear NMR spectroscopy. Science 252:1390–1399

Cornilescu G, Delaglio F, Bax A (1999) Protein backbone angle restraints from searching a database for chemical shift and sequence homology. J Biomol NMR 13(3):289–302

Culi J, Mann RS (2003) Boca, an endoplasmic reticulum protein required for wingless signaling and trafficking of LDL receptor family members in Drosophila. Cell 112:343–354

Culi J, Springer TA, Mann RS (2004) Boca-dependent maturation of beta-propeller/EGF modules in low-density lipoprotein receptor proteins. EMBO J 23:1372–1380

Delaglio F, Grzesiek S, Vuister GW, Zhu G, Pfeifer J, Bax A (1995) NMR pipe: a multidimensional spectral processing system based on UNIX pipes. J Biomol NMR 6:277–293

Garrett DS, Powers R, Gronenborn AM, Clore GM (1991) A common sense approach to peak picking two-, three- and four-dimensional spectra using automatic computer analysis of contour diagrams. JMagnReson 95:214–220

Guntert P (2004) Automated NMR structure calculation with CYANA. Methods Mol Biol 278:353–378

Herz J, Bock HH (2002) Lipoprotein receptors in the nervous system. Annu Rev Biochem 71:405–434

Hsieh JC, Lee L, Zhang L, Wefer S, Brown K, DeRossi C, Wines ME, Rosenquist T, Holdener BC (2003) Mesd encodes an LRP5/6 chaperone essential for specification of mouse embryonic polarity. Cell 112:355–367

Johnson BA (2004) Using NMR view to visualize and analyze the NMR spectra of macromolecules. Methods Mol Biol 278:313–352

Koduri V, Blacklow SC (2007) Requirement for natively unstructured regions of mesoderm development candidate 2 in promoting low-density lipoprotein receptor-related protein 6 maturation. Biochemistry 46:6570–6577

Kohler C, Andersen OM, Diehl A, Krause G, Schmieder P, Oschkinat H (2006) The solution structure of the core of mesoderm development (MESD), a chaperone for members of the LDLR-family. J Struct Funct Genomics 7:131–138

Laskowski RA, MacArthur MW, Moss DS, Thornton JM (1993) PROCHECK: a program to check the stereochemical quality of protein structures. J Appl Cryst 26:283–291

Li Y, Chen J, Lu W, McCormick LM, Wang J, Bu G (2005) Mesd binds to mature LDL-receptor-related protein-6 and antagonizes ligand binding. J Cell Sci 118:5305–5314

Strickland DK, Gonias SL, Argraves WS (2002) Diverse roles for the LDL receptor family. Trends Endocrinol Metab 13:66–74